phys. stat. sol. (c) **5**, No. 10, 3348–3352 (2008) / **DOI** 10.1002/pssc.200778879

physica status solidi c
www.pss-c.com
current topics in solid state physics

Influence of solution concentration and temperature on the aqueous chemical growth of zinc oxide structures

D. Vernardou[*,1,2,3], G. Kenanakis[1,2,4], K. Vlachou[3], E. Koudoumas[1,5], G. Kiriakidis[6], A. Vairis[7], and N. Katsarakis[1,2,6]

[1] Center of Materials Technology and Laser, School of Applied Technology, Technological Educational Institute of Crete, 710 04 Heraklion, Crete, Greece
[2] Science Department, School of Applied Technology, Technological Educational Institute of Crete, 710 04 Heraklion, Crete, Greece
[3] Department of Materials Science and Technology, University of Crete, 710 03 Heraklion, Crete, Greece
[4] Department of Chemistry, University of Crete, 710 03 Heraklion, Crete, Greece
[5] Department of Electrical Engineering, Technological Educational Institute of Crete, 710 04 Heraklion, Crete, Greece
[6] Institute of Electronic Structure and Laser, Foundation for Research & Technology-Hellas, P.O. Box 1527, Vassilika Vouton, 711 10 Heraklion, Crete, Greece
[7] Department of Mechanical Engineering, Technological Educational Institute of Crete, 710 04 Heraklion, Crete, Greece

Received 19 June 2007, revised 1 April 2008, accepted 3 April 2008
Published online 19 June 2008

PACS 61.05.cp, 68.37.Hk, 68.55.J-, 81.05.Dz, 81.16.Be

* Corresponding author: e-mail dimitra@iesl.forth.gr

ZnO was deposited on Corning glass using an equimolar aqueous solution of zinc nitrate hexahydrate and hexamethylenetetramine by Aqueous Chemical Growth. The morphological characteristics of the as-grown ZnO structures can be varied by adjusting the precursor solution concentration and solution temperature. An increase in the precursor solution concentration induces a modification in the ZnO morphology from sub-microrod to flower-like and microrod structures.

1 Introduction

ZnO is a versatile semiconductor with very interesting multi-functional properties. These properties find wide technological applications in photonic crystals [1], photodetectors [2], varistors [3], surface acoustic devices [4], sensors [5] and solar cells [6]. In order to improve the effectiveness of ZnO-based materials and to broaden the range of their applications, the control of their size and shape is a matter of considerable importance. As an example, the gas sensing capabilities of metal oxides have been observed to be improved with decreasing crystallite size and with increasing surface to volume ratio [7, 8]. Therefore, it is very important to investigate the possibility of influencing the growth mechanisms of ZnO towards the development of tailored morphological properties.

Nano- and microstructures such as wires or rods [9], tubes [10], coaxial cables [11], belts [12] and complex architectures based on various 1D structures (such as branches [13]) have attracted a great interest because they can provide opportunities to exploit novel properties and explore possible new phenomena. These diverse morphologies of ZnO have been developed using various mainly chemical processes such as chemical vapour deposition (CVD) [14], electrodeposition [15], spray pyrolysis [16], sol-gel [17] and Aqueous Chemical Growth (ACG) [9, 18, 19].

ACG is a quite simple, fast, low cost and environmental-friendly technique for the deposition of nano- and microstructures at relatively low temperatures. Moreover, the morphological characteristics of the grown samples could be tailored by controlling the solution chemistry (precipitation/dispersion conditions yielding to the thermodynamic stabilization of the system) by modifying the pH, the solution concentration and the solution temperature [20, 21].

Our recent studies have been focused on the solution of ZnO using the ACG technique for various deposition times, pH values and substrates [22, 23]. For microscope glass substrates, ZnO sponge-like structures were observed to transform into flower-like architectures with increasing deposition time, the size of the structures however, being non-uniform [22]. In the case of Corning glass, a modification of the ZnO morphology from rod-like to flower-like structures was achieved by varying the pH of the solution [23]. However, the layers were not compact due to the high precipitation rate, the structures also not having uniform size and shape.

In this work, we present a study on the influence of the solution concentration and solution temperature on the morphology of ZnO deposited on Corning glass by ACG. The scope of the study was a better understanding of the growth mechanisms towards the tailoring of the morphological characteristics of ZnO structures.

2 Experimental

The growth of ZnO was performed on Corning glass employing ACG, using concentrations of 10^{-3} M, 10^{-2} M and 10^{-1} M for various solution temperatures in the range of 80 to 100 ^{o}C. As precursor, an equimolar aqueous solution of $Zn(NO_3)_2{\cdot}6H_2O$ and HMTA was used. The solution was placed in Pyrex glass bottles with polypropylene autoclavable screw caps, the substrate positioned at the bottom, for 5 hr in a regular laboratory oven. After each induction period, the samples were thoroughly washed with MilliQ water in order to eliminate residual salts, and dried in air at a similar temperature with that used for the deposition.
X-ray Diffraction (XRD) measurements were performed using a Rigaku (RINT 2000) Diffractometer with CuKα X-rays for 2θ = 30.00-75.00^{o}. Scanning electron microscopy (SEM) was performed on a JEOL 840 electron microscope. Each characterization method was completed on at least three samples prepared under the same conditions as well as on different areas of the same samples for consistency and reproducibility.

3 Results and discussion

One way to affect the size and the shape of ZnO structures deposited on Corning glass by ACG is the control of the precipitation/dispersion rate by influencing the deposition parameters such as the solution concentration and solution temperature. Towards this scope, several ZnO samples were prepared at temperatures ranging from 80 ^{o}C to 100 ^{o}C and concentrations of 10^{-3} M, 10^{-2} M and 10^{-1} M. The deposition period was chosen to be 5 hr, due to the initial stage of the growth for shorter periods. The deposited ZnO samples were white in colour over the whole area of the substrate, for all deposition conditions. Moreover, samples appeared to have sufficient adhesion, passing the Scotch tape test. Finally, they were observed to be stable in air for over 6 months.

Figure 1 shows the XRD patterns of ZnO deposited on Corning for concentrations of 10^{-3} M, 10^{-2} M and 10^{-1} M at 90 ^{o}C for 5 hr. The "patterns" are consistent with the wurtzite ZnO hexagonal P6(3)mc structure according to JCPDS card file No. 36-1451. No other peaks were observed suggesting that single-phase ZnO was formed for the whole precursor concentration and solution temperature range used. In addition, the XRD patterns were identical all along the surface of the samples, i.e. no variations in the ZnO phase on the substrate area were observed.

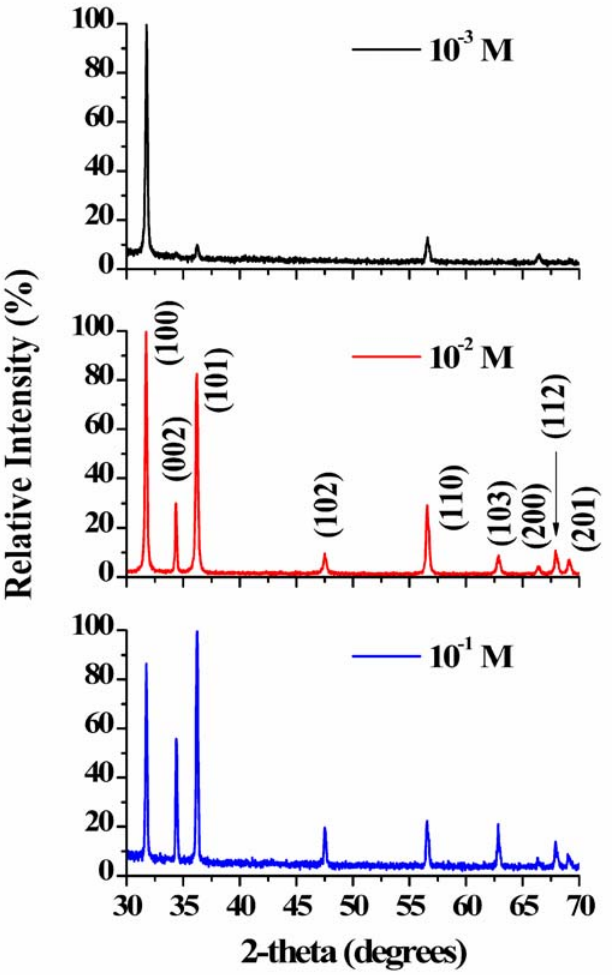

Figure 1 XRD analysis of ZnO grown on Corning glass using a 10^{-3} M, 10^{-2} M and 10^{-1} M solution concentration of $Zn(NO_3)_2{\cdot}6H_2O$ and HMTA at 90 ^{o}C for a deposition time of 5 hr.

SEM images of the ZnO grown using a solution concentration of 10^{-3} M at temperatures of 80, 90 and 100 ^{o}C are shown in Figs. 2(a), 2(b) and 2(c) respectively. Submicrorod and spindle-like ZnO structures of non-uniform size can be observed for all solution temperatures, the coverage of the substrate not overcoming ~65 %. The length of the structures increases from 6 μm up to 10 μm as the temperature rises from 80 ^{o}C to 100 ^{o}C. In contrast, their

diameter decreases respectively from 1-2 μm to 600 nm. Therefore, low precursor concentrations (10^{-3} M) favor the formation of sub-microrod and spindle-like structures, their size depending on solution temperature.

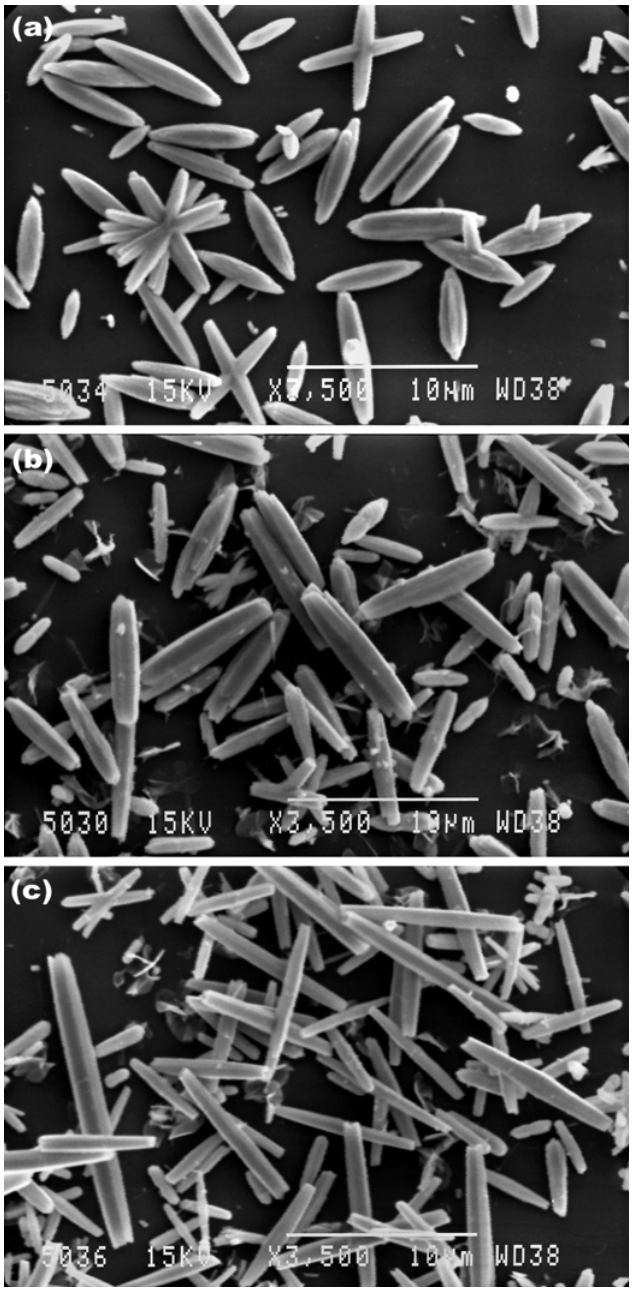

Figure 2 SEM images of ZnO deposited on Corning glass using ACG for a deposition time of 5 hr and solution concentration of 10^{-3} M at 80 °C (a), 90 °C (b) and 100 °C (c).

Figures 3(a), 3(b) and 3(c) present the SEM images of ZnO structures grown from a 10^{-2} M precursor solution at the same temperatures as above. For ≤90 °C, flower-like structures are observed, with only very few single rods present. At 80 °C, the flower-like structures consist of non-uniform rods with a mean diameter of 300-500 nm and a length of 3-4 μm (Fig. 3(a)). At 90 °C, the flower-like structures are of more uniform size and shape, while the substrate coverage increases to 85 % from ~60 % at 80 °C (Fig. 3(b)). Finally, at 100 °C, flower-like structures consisting of rods with a diameter of ~800 nm and a length of 8-9 μm are observed, while the substrate coverage reaches ~95 %. Consequently, the 10^{-2} M precursor concentration favors in general the formation of flower-like structures consisting of rods with length and diameter increasing with solution temperature.

Figures 3(d), 3(e) and 3(f) depict the SEM images of ZnO deposited from a 10^{-1} M precursor solution at 80 °C, 90 °C and 100 °C respectively. Non-uniform microrod structures can be seen in all cases, their exact size depending on the solution temperature. As the solution temperature increases from 80 °C to 100 °C the formation of more uniform microrods with larger dimensions (length of ~6-8 μm and diameter of 3-4 μm) is observed. Furthermore, the substrate coverage increases from ~70 % to ~90 %. Hence, the 10^{-1} M precursor concentration favors the formation of microrod structures, their dimensions varying with solution temperature. In any case, all structures have a hexagonal cross section, implying the occurrence of the wurtzite ZnO crystal structure as it was also demonstrated by XRD (Fig. 1).

Furthermore, it is interesting to note that the pH value of the solution after the growth was found to increase with temperature for all concentrations. As an example, for 10-1 M, the pH value increased from 7.56 to 7.96 as the solution temperature increased from 80 °C to 100 °C, indicating that there was no evaporation of ammonia. Therefore, there was enough base left in the solution to react with zinc nitrate (see reactions 1-4 below [20, 24]), which did not restrict the growth of the structures as confirmed from the SEM images of Fig. 3.

$$(CH_2)_6N_4 + 6H_2O \rightarrow 6HCHO + 4NH_3, \quad (1)$$

$$NH_3 + H_2O \rightarrow NH_4^+ + OH^-, \quad (2)$$

$$Zn^{2+} + 2OH^- \rightarrow Zn(OH)_{2\,(l)}, \quad (3)$$

$$Zn(OH)_{2\,(s)} \rightarrow ZnO_{\,(s)} + H_2O. \quad (4)$$

The morphology of ZnO structures is altered by the solution concentration and temperature during the deposition process, which they can consequently affect the nucleation and growth processes in aqueous solution [25]. Hence for 10^{-3} M solution concentration and solution temperature at 100 °C, ZnO nuclei may aggregate together and grow along the x-axis into rod-like crystals (Fig. 1 and Fig. 2). As the concentration increases further to 10^{-2} M the nucleation of ZnO is faster and hence more nuclei can be formed in the initial stage [25]. Each of them can individually grow along the x and z-axes, resulting in flower-like structures (Fig. 1 and Figs. 3(a)-(c)). At a yet higher concentration of 10^{-1} M, much more nuclei are generated and aggregated to grow into microrod structures. This may come from an attachment process of flower-like structures closely packed together.

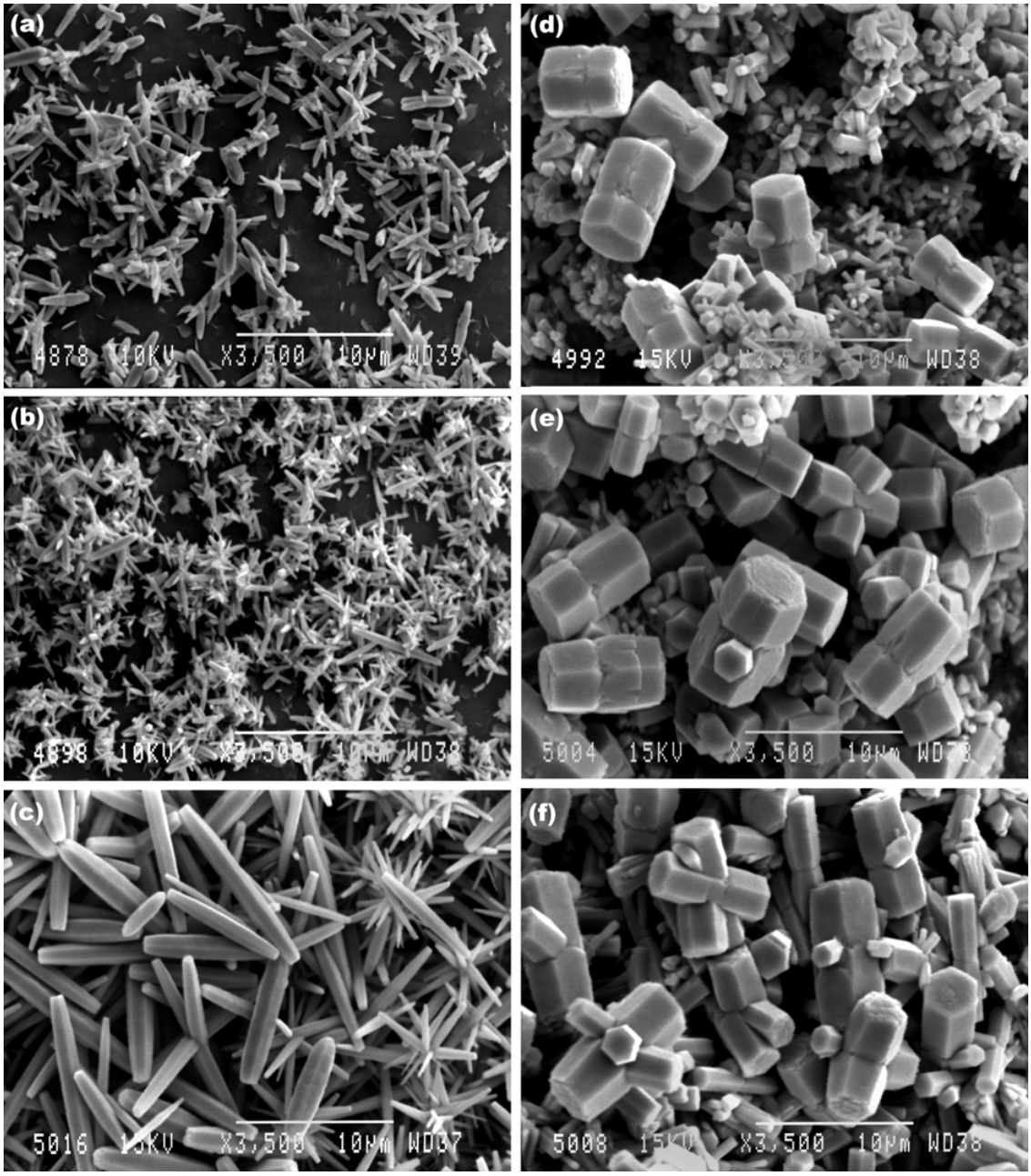

Figure 3 SEM images of ZnO deposited on Corning glass using ACG for a deposition time of 5 hr and solution concentration of 10^{-2} M at 80 °C (a), 90 °C (b) and 100 °C (c) and of 10^{-1} M at 80 °C (d), 90 °C (e) and 100 °C (f).

The attachment process is thermodynamically favourable since the surface energy is significantly reduced due to the elimination of the interface [25]. Penn and Banfield have observed similar phenomenon where smaller structures undergo attachment or coalescence to form larger dimension structures [26, 27]. However, it is necessary to perform further studies in order to unambiguously identify the mechanism that operates for these particular ACG processes.

It can be finally noticed that the ZnO samples grown from a 10^{-2} M precursor solution at 90 °C and 100 °C show efficient substrate coverage (~85-95 %) and high surface-to-volume ratio, which might drastically improve the effectiveness of ZnO for gas sensing applications.

4 Conclusions

ZnO structures with different morphology, such as submicrorod, flower-like and microrod structures have been synthesized by ACG. It has been found that the shape and

size of the structures strongly depend on the concentration and the temperature of the precursor solution. It may be concluded that ZnO structures with high surface-to-volume ratio and efficient substrate coverage could be potentially suitable for gas sensing applications.

Acknowledgements This work was co financed by 75% from the European Social Fund (ESF) and by 25% from national Greek resources (ARCHIMIDIS II). Furthermore, the authors would like to thank Mrs Aleka Manousaki for SEM measurements.

References

[1] Y. Chen, D. Bagnall, and T. Yao, Mater. Sci. Eng. B **75**, 190 (2000).
[2] S. Liang, H. Sheng, Y. Liu, Z. Hio, Y. Lu, and H. Shen, J. Cryst. Growth **225**, 110 (2001).
[3] M. H. Koch, P. Y. Timbrell, and R. N. Lamb, Semicond. Sci. Technol. **10**, 1523 (1995).
[4] C. R. Gorla, N. W. Emanetoglu, S. Liang, W. E. Mayo, Y. Lu, M. Wraback, and H. Shen, J. Appl. Phys. **85**, 2595 (1999).
[5] J. F. Chang, H. H. Kuo, I. C. Leu, and M. H. Hon, Sens. Actuators B **84**, 258 (2002).
[6] H. Rensmo, K. Keis, H. Lindström, S. Södergren, A. Solbrand, A. Hagfeldt, S.-E. Lindquist, L. N. Wang, and M. Muhammed, J. Phys. Chem. B **101**, 2598 (1997).
[7] N. Yamazoe, Sens. Actuators B **5**, 7 (1991).
[8] A. Gurlo, N. Barsan, M. Ivanovskaya, U. Weimar, and W. Gopel, Sens. Actuators B **47**, 92 (1998).
[9] L. Vayssieres, Adv. Mater. **15**, 464 (2003).
[10] L. Vayssieres, K. Keis, A. Hagfeldt, and S.-E. Lindquist, Chem. Mater. **13**, 4395 (2001).
[11] J. Q. Hu, Q. Li, X. M. Meng, C. S. Lee, and S. T. Lee, Chem. Mater. **15**, 305 (2003).
[12] Z. W. Pan, Z. R. Dai, and Z. L. Wang, Science **291**, 1947 (2001).
[13] V. A. L. Roy, A. B. Djurisic, W. K. Chan, J. Gao, H. F. Lui, and C. Surya, Appl. Phys. Lett. **83**, 141 (2003).
[14] J. J. Wu and S. C. Liu, Adv. Mater. **14**, 215 (2002).
[15] B. Illy, B. A. Shollock, J. L. MacManus-Driscoll, and M. P. Ryan, Nanotechnology **16**, 320 (2005).
[16] S. A. Studenkin, N. Golego, and M. Cocivera, J. Appl. Phys. **83**, 2104 (1998).
[17] M. Ohyama, H. Kozuka, and T. Yoko, Thin Solid Films **306**, 78 (1997).
[18] Q. Li, V. Kumar, Y. Li, H. Zhang, T. J. Marks, and R. P. H. Chang, Chem. Mater. **17**, 1001 (2005).
[19] X. Liu, Z. Jin, S. Bu, J. Zhao, and K. Yu, Mater. Sci. Eng. B **129**, 139 (2006).
[20] L. Vayssieres, Int. J. Nanotechnology **1**, 1 (2004).
[21] H. Zhang, D. Yang, S. Li, X. Ma, Y. Ji, J. Xu, and D. Que, Mater. Lett. **59**, 1696 (2005).
[22] G. Kenanakis, D. Vernardou, E. Koudoumas, G. Kiriakidis, and N. Katsarakis, Sens. Actuators B **124**, 187 (2007).
[23] D. Vernardou, G. Kenanakis, S. Couris, E. Koudoumas, E. Kymakis, and N. Katsarakis, Thin Solid Films **515**, 8764 (2007).
[24] S. Yamabi and H. Imai, J. Mater. Chem. **12**, 3773 (2002).
[25] W. Peng, S. Qu, G. Cong, and Z. Wang, J. Cryst. Growth **6**, 1518 (2006).
[26] J. F. Banfield, S. A. Welch, H. Zhang, T. T. Ebert, and R. L. Penn, Science **289**, 751 (2000).
[27] R. L. Penn and J. F. Banfield, Science **281**, 969 (1998).

